

# A Nano-Combinatorial Library Strategy for the Discovery of Nanotubes with Reduced Protein-Binding, Cytotoxicity, and Immune Response

Hongyu Zhou,<sup>†‡</sup> Qingxin Mu,<sup>†‡</sup> Ningning Gao,<sup>‡</sup> Aifeng Liu,<sup>‡</sup> Yuehan Xing,<sup>‡</sup>  
Sulian Gao,<sup>‡</sup> Qiu Zhang,<sup>‡</sup> Guangbo Qu,<sup>‡</sup> Yuyan Chen,<sup>§</sup> Gang Liu,<sup>§</sup>  
Bin Zhang,<sup>‡</sup> and Bing Yan<sup>\*,†‡</sup>

*St. Jude Children's Research Hospital, Memphis, Tennessee 38105, School of Pharmaceutical Sciences, Shandong University, Jinan, China, and Institute of Materia Medica, Chinese Academy of Medical Sciences, Beijing, China*

*Received November 19, 2007; Revised Manuscript Received January 15, 2008*

## ABSTRACT

We have discovered functionalized multiwalled carbon nanotubes with reduced protein-binding, cytotoxicity, and immune response and the associated structure–activity relationships using *in silico* surface molecular diversity design, combinatorial library synthesis, and multiple biological screenings. Our results demonstrated the general utility of the nanocombinatorial library approach in nanomedicine and nanotoxicity research.

Carbon nanotubes have been widely studied for their potential applications in biology<sup>1</sup> and medicine.<sup>2</sup> When injected into an animal, they enter various organs<sup>3,4</sup> and cellular compartments<sup>5–8</sup> and bind to protein<sup>9,10</sup> and DNA<sup>11</sup> molecules. These properties offer functionalized nanotubes tremendous opportunities to function as intracellular probes, drug carriers, imaging agents, DNA modulators, and other medical devices on the condition that they are biocompatible. The bioactivity of a nanomaterial is modulated by its surface chemistry,<sup>12–20</sup> among other factors.<sup>14,21–30</sup> By attaching copies of a molecule on single-walled carbon nanotubes, their cellular interactions were noticeably altered.<sup>6,31–34</sup> Multiple reagents were used to more efficiently assemble a collection of surface modified magnetic nanoparticles and assisted in selecting particles with the best biological property.<sup>35–39</sup> Combinatorial modifications of the nanotube's surface would enable us to map unknown chemical space more effectively and to rapidly discover nanotubes with reduced toxicity and reveal structure–activity relationships at the same time.

To discover biocompatible nanotubes without *a priori* knowledge of the related targets, we decided to expose these

targets with the maximum surface structural diversity of nanotubes through combinatorial nanotube library synthesis (Figure 1). Chemical diversity of the surface molecules relies on the diversity of the building blocks used to make these molecules. We first set out to select highly diverse building blocks by carrying out calculations of 31 amines and 26 acylators for their estimated molecular properties such as similarities, hydrophobicity, solubility, topological, and stereochemical properties using Accord and Pipeline Pilot from Accelrys (Table S1 in the Supporting Information). Eight amines and nine acylators (Figure 2) were selected for library synthesis. This designed nanotube library contained 80 f-MWNTs (8 × 10; eight amines, nine acylators, and one without acylation), and their surface molecules have the most diverse molecular and physicochemical properties on the basis of the computation (Figure S1 in Supporting Information).

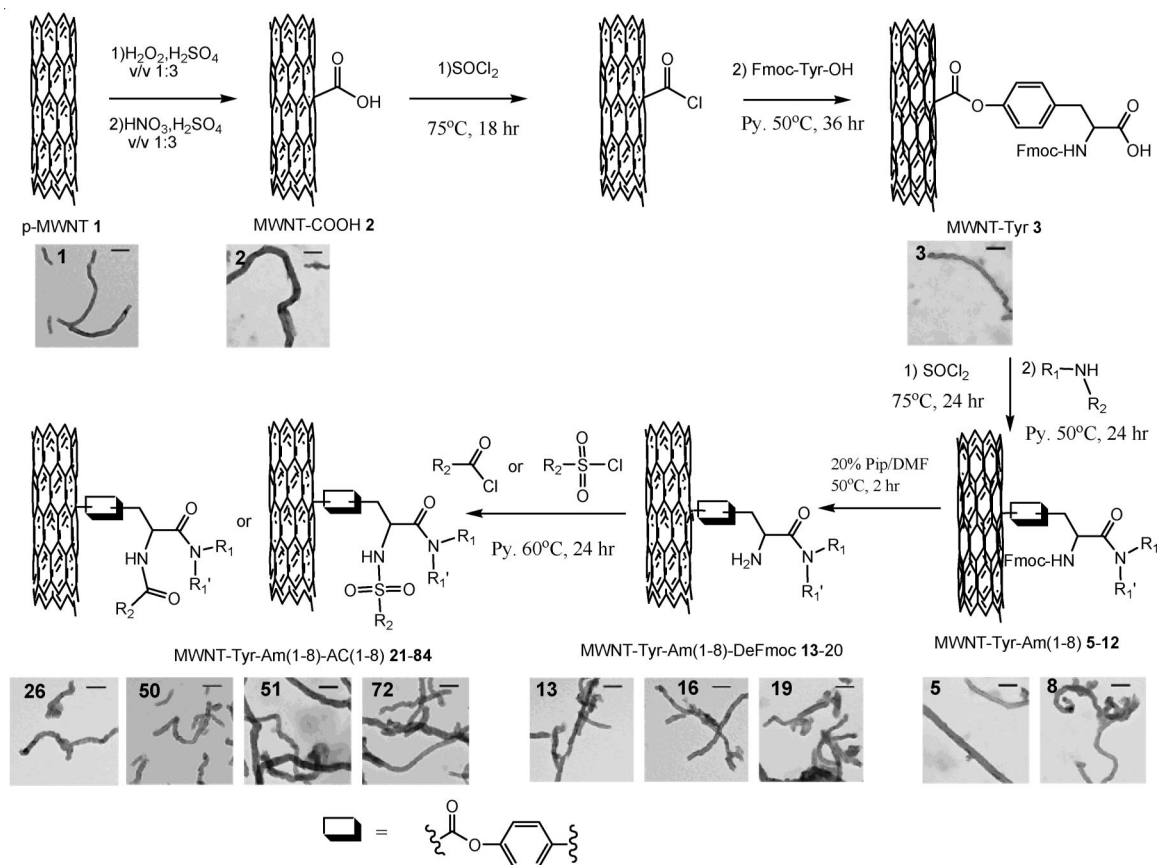
Pristine MWNT **1** was first oxidized to MWNT-COOH **2** by an optimized two-step oxidation protocol (see Supporting Information). Under the oxidation conditions we used, carboxyl groups should be formed along the nanotube sidewalls in addition to at its termini.<sup>40</sup> MWNT-COOH **2** then reacted with a 10-fold excess of Fmoc-protected tyrosine to form **3**. The loading of carboxyl groups in **2** was quantified by elemental analysis of **3** for its nitrogen content (0.45 ± 0.01 mmol/g) and by quantification of the released Fmoc groups during the generation of **4** (0.41 ± 0.03 mmol/g).

\* Corresponding author. E-mail: bing.yan@stjude.org. Telephone: +9014952797. Fax: +9014955715.

<sup>†</sup> St. Jude Children's Research Hospital.

<sup>‡</sup> School of Pharmaceutical Sciences, Shandong University.

<sup>§</sup> Institute of Materia Medica.

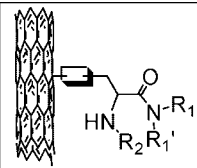
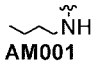
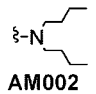
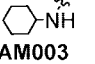
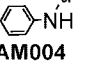
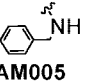
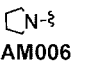
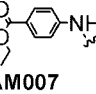
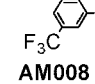
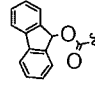
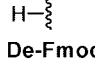
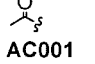
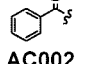
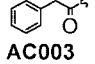
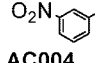
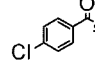
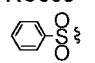
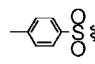
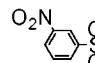


**Figure 1.** Synthesis route of the f-MWNT library and selected transmission electron microscopy images of f-MWNTs. The bar in each photo represents a length of 100 nm.

Because we had no direct evidence that the reaction yield between **2** and Fmoc-Tyr is 100%, the above values should be a lower limit of the carboxyl group loading. Using **3** as a starting point, a nanotube library with two dimensions of diversification was synthesized (Figure 1). We applied multiple strategies to ensure the library was successfully synthesized, purified, and well characterized. These strategies include the following: (1) applying robust reactions for library generation, (2) optimizing reaction conditions for each step, (3) purifying reaction products and intermediates, and (4) developing liquid chromatography method for monitoring the effectiveness of purification (Figures 3a and 5) characterizing reaction products and intermediates by applying magic-angle spinning proton nuclear magnetic resonance spectroscopy (MAS  $^1\text{H}$  NMR) analysis (Figure 3c), Fourier transform infrared spectroscopy (FTIR Figure 3b), elemental analysis (Table S2 in Supporting Information), and Fmoc quantification methods.

NMR is the gold standard for identifying the structures of organic molecules. However, NMR of f-MWNTs showed no detectable signals due to the line broadening induced by magnetic susceptibility differences from their heterogeneity. It has long been recognized that the magnetic-susceptibility-induced line broadenings in heterogeneous samples can be eliminated by spinning the sample at the magic angle ( $54.7^\circ$  from  $Z$ ).<sup>41,42</sup> In this investigation, we used MAS  $^1\text{H}$  NMR with a nanoprobe to acquire  $^1\text{H}$  NMR spectra of nanoparticle-bound molecules for their characterizations (Figure 3c).

Because we were unable to suspend MWNT **1** in the NMR solvent, its  $^1\text{H}$  NMR spectrum was not obtained. The MAS  $^1\text{H}$  NMR spectrum of MWNT-COOH **2** (top spectrum in Figure 3c) showed signals of NMR solvent DMSO- $d_6$  at 2.5 ppm, water at 3.33 ppm, and a number of small NMR signals, possibly from hydroxyl groups and some defect sites. We also acquired  $^1\text{H}$  NMR spectra of 12 other f-MWNT library members. Samples were selected in such a way that each sample shared a building block with another sample in the selection. MAS  $^1\text{H}$  NMR spectra of nanoparticle-bound molecules are very different from solution-phase NMR spectra in coupling and splitting properties while the chemical shift remains the same. F-MWNTs **26** and **50** were incorporated identical acylators, but different amines (*n*-butylamine in **26** and aniline in **50**). This difference was reflected by an extra signal at 7.6 ppm in the  $^1\text{H}$  NMR spectrum of **50** (Figure 3). F-MWNTs **26** and **50** had a benzenesulfonyl group in their surface molecules, and f-MWNTs **28** and **76** had nearly identical surface molecules except they had a 3-nitro-benzenesulfonyl group instead. The existence of the nitro group reduced the electron density of the phenyl ring and caused a downfield shift for aromatic protons in **28** and **76** (7.64–8.71) compared with those in **26** and **50** (7.29–7.94). Through analysis of chemical shifts and signal ratios, we positively confirmed molecules bound to nanotubes. Combining with the reaction progression monitoring by FTIR (Figure 3b) and the quantitative loading analysis throughout

		$R_1R_1'N-$							
		 AM001	 AM002	 AM003	 AM004	 AM005	 AM006	 AM007	 AM008
R2-	 Fmoc	5	6	7	8	9	10	11	12
	 De-Fmoc	13	14	15	16	17	18	19	20
	 AC001	21	29	37	45	53	61	69	77
	 AC002	22	30	38	46	54	62	70	78
	 AC003	23	31	39	47	55	63	71	79
	 AC004	24	32	40	48	56	64	72	80
	 AC005	25	33	41	49	57	65	73	81
	 AC006	26	34	42	50	58	66	74	82
	 AC007	27	35	43	51	59	67	75	83
	 AC008	28	36	44	52	60	68	76	84

**Figure 2.** Surface molecular compositions of combinatorial MWNT library members.

the reaction sequence by elemental analysis of selected f-MWNTs (Table S2 in Supporting Information), the library was characterized.

To confirm the morphological integrity of MWNTs after multiple reaction steps, pristine MWNT **1**, intermediate MWNTs **2** and **3**, and f-MWNT library members **5**, **8**, **13**, **16**, **19**, **26**, **28**, **50**, **51**, **72**, and **76** were characterized by transmission electron microscopy (TEM) (Figure 1), which showed that there has been no change of the gross MWNT structure throughout the reaction sequence. In this way, we ensured that combinatorial chemistry modifications were mainly affecting surface properties, while the size and shape of f-MWNTs remained unperturbed. Sonication of f-MWNTs in water yielded black suspensions that were stable for 10 h before precipitation. When we soaked f-MWNTs in water for two days and sonicated the mixture, stable suspensions were formed and were stable at 24 °C for two months (Figure S2 in Supporting Information).

Surface dominant nanotubes have a strong tendency to bind proteins.<sup>9,10,13,16,21,43,44</sup> Protein binding increases a nanoparticle's propensity to be opsonized<sup>44–46</sup> for clearance or to create cryptic epitopes in cellular signaling proteins causing

toxic responses. To determine whether the surface modifications on f-MWNTs could alter or, hopefully, reduce their protein-binding tendency, we investigated the interactions of f-MWNTs with a representative subset of proteins (BSA, carbonic anhydrase, chymotrypsin, and hemoglobin) with various functions. The binding of f-MWNTs to these proteins were studied by steady-state fluorescence spectroscopy. Protein intrinsic fluorescence was quenched by f-MWNTs, indicating molecular interactions between f-MWNT and proteins. Results showed that diverse surface chemistry significantly altered protein-binding capabilities of f-MWNTs compared with MWNT-COOH **2**, which was the precursor of the library (Figure 4). Proteins maintained their secondary structures after binding to nanotubes according to our CD studies.<sup>47</sup> From the assay results, we found that acylator AC005 generated surface molecules that produced much less protein binding in all assays.

The protein-binding ability of f-MWNTs can also be determined by light sonication of a mixture of nanotubes and proteins because protein bindings can solubilize otherwise insoluble nanotubes.<sup>48</sup> We treated the library in cell culture medium containing 10% heat-inactivated horse serum.

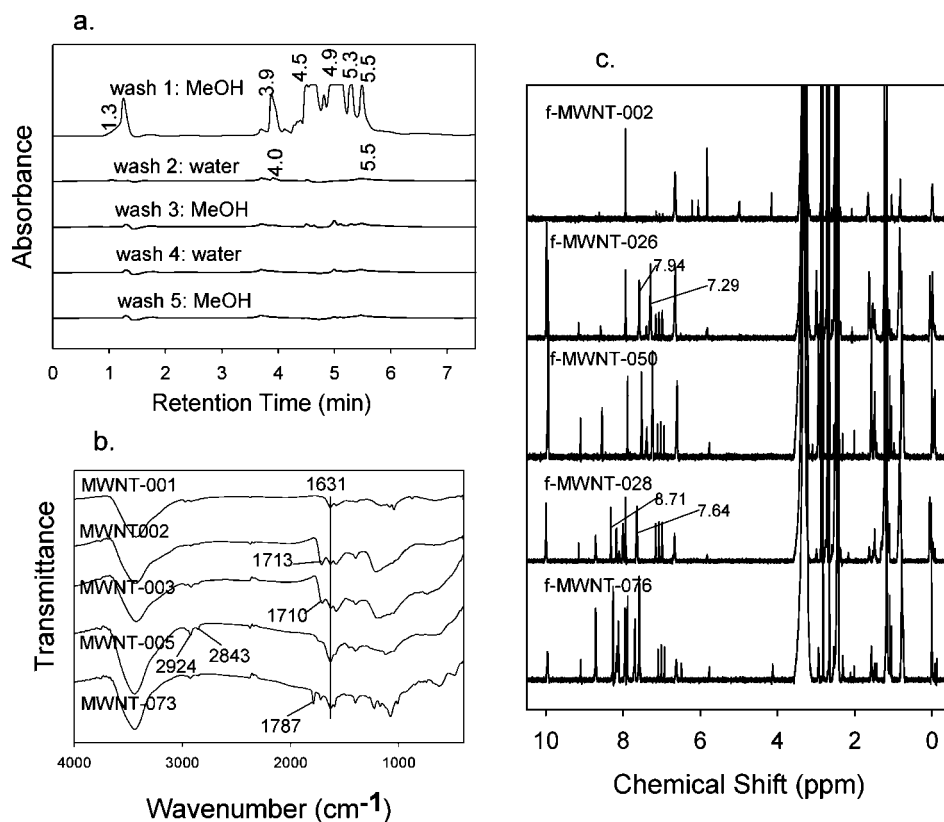


**Figure 3.** Analysis, purification, and characterization of f-MWNTs. (a) LC/MS analysis after alternative solvent (EtOH and water) wash and centrifugation to monitor the effectiveness of purification during the synthesis of f-MWNT **31**. (b) IR spectra of f-MWNTs **1**, **2**, **3**, **5**, and **73**. When pristine MWNT was oxidized, an IR band at  $1713\text{ cm}^{-1}$  appeared indicating the formation of carboxylic acid groups. MWNT **2** reacted with Fmoc-Tyr and the IR bands of phenol ester carbonyl and carboxylic acid of tyrosine overlapped at  $\sim 1710\text{ cm}^{-1}$ . The amidation of **3** produced **5**, which was characterized by disappearance of an acid carbonyl band at  $1710$  and the formation of bands at  $2843$  and  $2924\text{ cm}^{-1}$ . Final product synthesis induced further IR changes. In the case of f-MWNT **73**, an ester carbonyl band at  $1787\text{ cm}^{-1}$  was formed due to an ester group on one of its building blocks. (c) MAS  $^1\text{H}$  NMR of f-MWNTs **2**, **26**, **50**, **28**, and **76**.

All f-MWNTs immediately formed uniform black suspension after a 3 min sonication except f-MWNTs **18**, **25**, **41**, **57**, and **73**. These f-MWNTs could not be suspended due to their poor protein bindings. After two days, six more f-MWNTs, **20**, **33**, **49**, **65**, **80**, and **82**, also became less soluble (Figure S3 in Supporting Information). Noticeably, 7 out of 11 protein evaders contained acylator building block AC005. Although these f-MWNTs had surface molecules barely different from those of protein-binding f-MWNTs (Figure 2), they effectively avoided protein binding. We next examined the binding of 24 f-MWNTs with hundreds of proteins in human plasma.<sup>49</sup> Among 24 f-MWNTs (Figure 2) tested, eight had surface molecules that contained building block AC005 (**25**, **33**, **41**, **49**, **57**, **65**, **73**, and **81**), eight contained AC002 (**22**, **30**, **38**, **46**, **54**, **62**, **70**, and **78**) that had the highest structural similarity to AC005 (Figure S3 in Supporting Information), and eight contained Fmoc groups (**5**, **6**, **7**, **8**, **9**, **10**, **11**, and **12**). All f-MWNTs that had surface molecules containing AC005 with the exception of **65** showed no protein binding and remained insoluble with a 3 min sonication (Figure S4 in Supporting Information), but the others were well suspended and remained in suspension for at least seven days.

Surface-bound molecules containing building blocks AC005 or AC002 had amazingly similar hydrophobicity, stereochemical, and hydrogen-bonding properties on the basis of

computation. Zeta potential measurements (Figure S4 in Supporting Information) showed that their  $\zeta$  potentials are also comparable, indicating their similar surface electrostatic properties. Therefore, the protein evading nature of f-MWNTs that had AC005 containing molecules was solely due to a unique structural feature of AC005: a single atom switching from H to Cl at the 4-position of the benzene ring compared with AC002 rather than other conceivable abnormalities. These findings provided compelling evidence that AC005 is a key building block that constitutes surface molecules with a significantly protein-rejecting ability.

The general altered protein binding activities of the f-MWNT library indicated that nanotubes may perturb the normal cellular functions such as cell viability and immune responses. Nonadherent monocytes, THP-1 cells, differentiated into macrophages after the addition of phorbol 12-myristate 13-acetate at a concentration of  $50\text{ ng/mL}$  and incubation for 48 h. Differentiated cells were characterized by their adherence to the plastic well surface in 96-well plates after the removal of the nonadherent monocytes. To avoid the artifactual interference from MTT assay, we used the WST-1 assay<sup>50</sup> to evaluate the acute cytotoxicity of the f-MWNT library in macrophages. The assay measures the viability of cells by determining the activity of the mitochondrial dehydrogenases (Figure 5a,b). Results showed that depending on the surface chemistry of the f-MWNTs, they

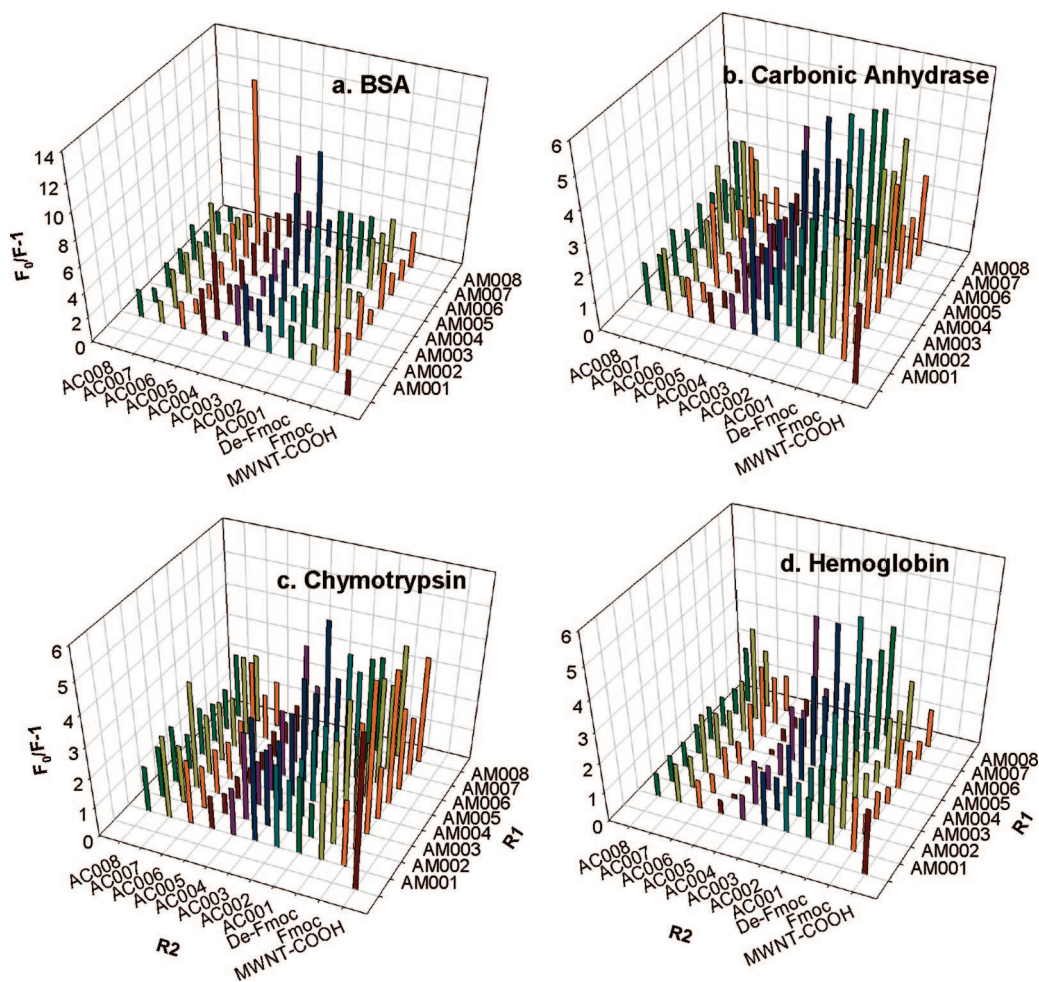


**Figure 4.** Protein binding of the f-MWNT library. (a) BSA, (b) carbonic anhydrase, (c) chymotrypsin, and (d) hemoglobin were used in an f-MWNTs/protein binding assay. The binding affinity of library members was compared with the degree of binding of MWNT-COOH. R1 represents amine building blocks, and R2 represents acylator building blocks. Three f-MWNT concentrations (0.0, 7.5, and 15.0  $\mu\text{g/mL}$ ) were used in fluorescence titration, and  $F_0/F$  for 15  $\mu\text{g/mL}$  f-MWNT was plotted as vertical bars.

**Table 1.** Multiassay Scores for Top 30 f-MWNTs<sup>a</sup>

f-MWNT	BSA binding	CA binding	CT binding	HB binding	cell viability	NO response	multiassay score	f-MWNT	BSA binding	CA binding	CT binding	HB binding	cell viability	NO response	multiassay score
40	6	23	18	18	3	12	80	11	17	36	37	11	9	57	167
<b>57</b>	43	7	2	3	16	16	87	17	3	21	33	14	71	28	170
<b>49</b>	38	1	1	1	21	27	89	60	47	29	26	34	17	19	172
<b>65</b>	37	9	7	7	18	20	98	48	14	43	24	31	25	42	179
82	5	14	22	39	27	3	110	<b>73</b>	49	6	4	6	49	65	179
68	11	25	13	27	11	25	112	1	2	11	8	5	76	78	180
52	29	15	11	26	37	2	120	34	8	3	15	12	79	64	181
50	25	5	12	15	23	41	121	38	31	56	36	35	13	10	181
64	15	19	27	41	8	13	123	16	36	32	38	19	20	38	183
44	28	30	34	20	4	8	124	28	35	24	21	17	65	26	188
<b>41</b>	16	8	5	4	59	37	129	<b>25</b>	66	12	9	8	19	75	189
42	10	58	19	29	1	18	135	36	7	18	29	23	73	40	190
<b>33</b>	77	2	3	2	48	9	141	35	53	4	35	28	36	35	191
8	9	26	32	9	66	4	146	24	1	17	25	21	80	51	195
<b>81</b>	26	13	6	10	75	31	161	51	51	31	40	51	22	1	196

<sup>a</sup> f-MWNTs showing in bold and underlined all contained AC005.

exhibited quite different cytotoxicity compared with the cell viability induced by the precursor, MWNT-COOH **2**. Many f-MWNTs generated higher cell viability compared to **2** at both low and high nanotube concentrations.

Macrophages, when activated, phagocytose foreign nanoparticles and secrete chemical mediators of inflammation such as nitric oxide (NO).<sup>51</sup> To measure the immune response, macrophages were treated with f-MWNTs for 24 h in the

presence of lipopolysaccharide (LPS, 100 ng/mL). The nitrite concentration was then determined as an indicator for NO generation<sup>52</sup> and the induction of the inducible NO synthase. Compared with the control (only 100 ng/mL LPS added), 33 f-MWNTs showed reduced NO generation at a low nanotube concentration (50  $\mu\text{g/mL}$ ) (Figure 5c). Although a generally higher NO generation was found at a higher f-MWNT concentration (200  $\mu\text{g/mL}$ , Figure 5d), there were

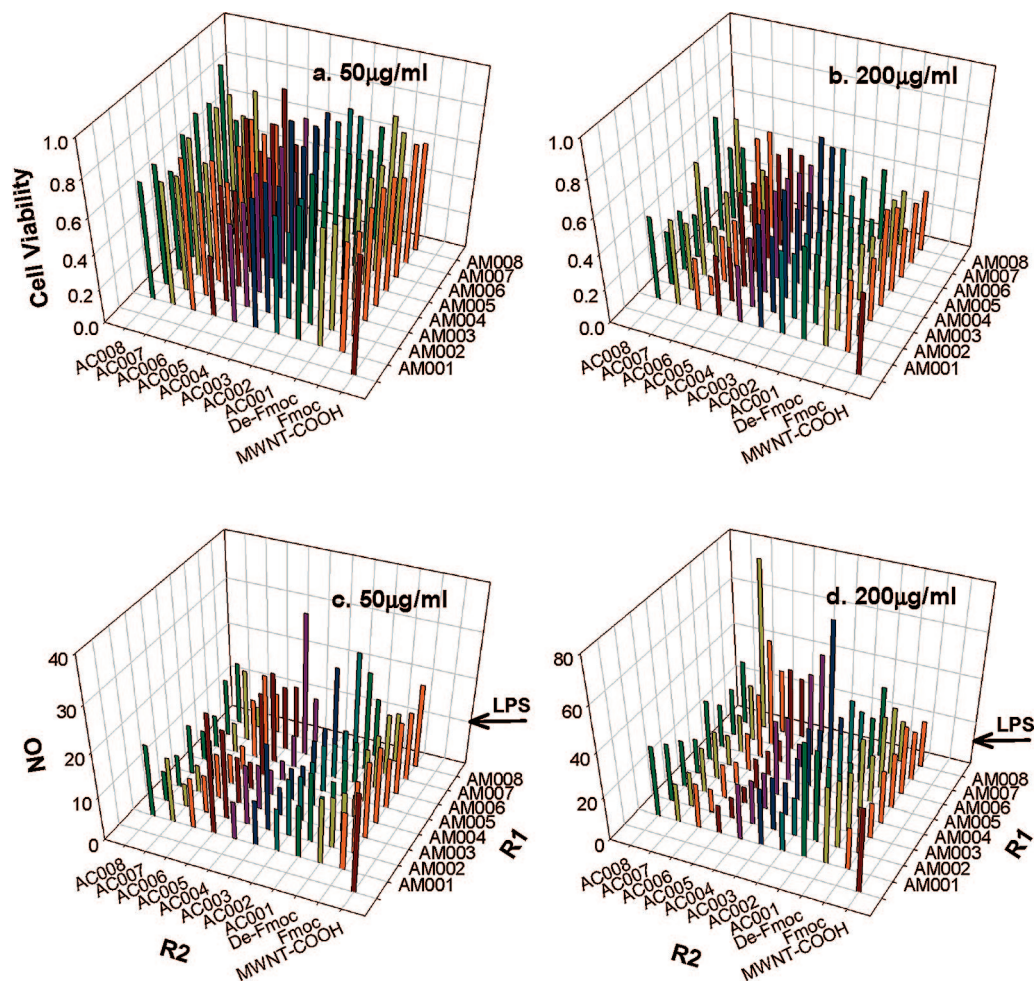


**Figure 5.** Cytotoxicity and immune responses induced by the f-MWNT library. Library members were assayed for their cytotoxicity (a and b) in THP-1 cells and MWNT-induced NO release (c and d) at either 50  $\mu\text{g/mL}$  (a and c) or 200  $\mu\text{g/mL}$  (b and d). The fractions of viable cells after incubation with f-MWNTs for 24 h are shown as vertical bars in (a) and (b). The basal level of NO release by LPS (100 ng/mL) is marked on panels (c) and (d). The f-MWNT library-induced NO release in the presence of LPS (100 ng/mL) is shown as vertical bars.

still six f-MWNTs showing NO responses similar to or lower than those of the control.

To select suitable candidates for further lead optimization, we analyzed results from all assays (Table 1, Figure 6). The results from four protein binding assays, nitric oxide generation, and the cytotoxicity assay were each ranked from 1 to 80 for all f-MWNTs (smaller number means lower binding, higher cell viability and lower NO generation). The sum of an f-MWNT's rankings was designated its multiassay score. A smaller multiassay score was deemed superior in terms of overall biocompatibility. The f-MWNTs **40**, **57**, **49**, and **65** have scores less than 100 in a possible score range of 6–480, showing that they are suitable candidates for further optimization. A remarkable structure–activity relationship was also revealed in this study. Three out of the top five lead candidates contained the building block AC005, and all eight AC005-containing f-MWNTs in the library were in the top 26 multiassay scores. Examining the least biocompatible (or higher score) f-MWNTs in Table 1, AC001, AC003, AM005, AM007, and AM008 each generated 4–5 f-MWNTs that have multiassay scores at the

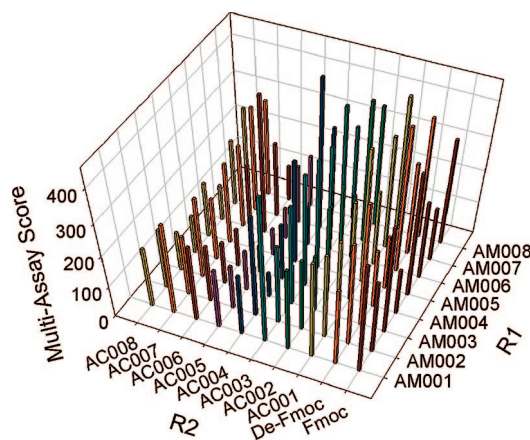


**Figure 6.** Multiassay score of the f-MWNT library. Findings from four protein binding assays, cytotoxicity, and immune response assays (at 50  $\mu\text{g/mL}$ ) were ranked for all library members. The sum of their ranks was designated the multiassay score and is shown as vertical bars in the graph.

bottom 30, suggesting that these building blocks generated surface molecules that made less biocompatible nanotubes.

In summary, we have made a novel surface-modified MWNT library containing 80 members and identified novel f-MWNTs with reduced protein binding, cytotoxicity, and immune responses using in silico design, combinatorial synthesis, and multiple biological screenings. We also discovered that AC005 is required for generating surface molecules that confer better biocompatibility in nanotubes. Our approach is more effective in mapping chemical space governing nanotube biocompatibility and discovering lead structure. At the same time, structure–activity and structure–toxicity relationship was also obtained. The rapid discovery of four leading candidates and their associated structure–activity relationships demonstrated the general utility of the nanocombinatorial library approach in nanomedicine and nanotoxicity research.

**Acknowledgment.** We thank Dr. Shumei Zhai, Ying Zhang, Fang Wang, and Ying Sun from Shandong University for their technical assistance and Sharon Frase (University of Memphis and St. Jude Children’s Research Hospital) for acquiring transmission electron microscopic images. This work was supported by the American Lebanese and Syrian Associated Charities (ALSAC), St. Jude Children’s Research Hospital, and Shandong University.

**Supporting Information Available:** Experimental details, calculated physicochemical properties of the entire virtual f-MWNT library, elemental analysis of selected f-MWNTs in the synthesized f-MWNT library, and total protein binding assay results for the library in cell culture medium and human plasma. This material is available free of charge via the Internet at <http://pubs.acs.org>.

## References

- (1) Mattson, M. P.; Haddon, R. C.; Rao, A. M. *J. Mol. Neurosci.* **2000**, *14*, 175–182.
- (2) Liu, Z.; Cai, W. B.; He, L. N.; Nakayama, N.; Chen, K.; Sun, X. M.; Chen, X. Y.; Dai, H. J. *Nat. Nanotechnol.* **2007**, *2*, 47–52.
- (3) Singh, R.; Pantarotto, D.; Lacerda, L.; Pastorin, G.; Klumpp, C.; Prato, M.; Bianco, A.; Kostarelos, K. *Proc. Natl. Acad. Sci. U.S.A.* **2006**, *103*, 3357–3362.
- (4) Wang, H. F.; Wang, J.; Deng, X. Y.; Sun, H. F.; Shi, Z. J.; Gu, Z. N.; Liu, Y. F.; Zhao, Y. L. *J. Nanosci. Nanotechnol.* **2004**, *4*, 1019–1024.
- (5) Cherukuri, P.; Bachilo, S. M.; Litovsky, S. H.; Weisman, R. B. *J. Am. Chem. Soc.* **2004**, *126*, 15638–15639.
- (6) Kam, N. W. S.; Dai, H. J. *J. Am. Chem. Soc.* **2005**, *127*, 6021–6026.
- (7) Kam, N. W. S.; Jessop, T. C.; Wender, P. A.; Dai, H. J. *J. Am. Chem. Soc.* **2004**, *126*, 6850–6851.
- (8) Pantarotto, D.; Briand, J. P.; Prato, M.; Bianco, A. *Chem. Commun.* **2004**, 16–17.
- (9) Karajanagi, S. S.; Vertegel, A. A.; Kane, R. S.; Dordick, J. S. *Langmuir* **2004**, *20*, 11594–11599.
- (10) Lin, Y.; Allard, L. F.; Sun, Y. P. *J. Phys. Chem. B* **2004**, *108*, 3760–3764.
- (11) Zheng, M.; Jagota, A.; Semke, E. D.; Diner, B. A.; McLean, R. S.; Lustig, S. R.; Richardson, R. E.; Tassi, N. G. *Nat. Mater.* **2003**, *2*, 338–342.
- (12) Chen, X.; Tam, U. C.; Czapinski, J. L.; Lee, G. S.; Rabuka, D.; Zettl, A.; Bertozzi, C. R. *J. Am. Chem. Soc.* **2006**, *128*, 6292–6293.
- (13) Colvin, V. L.; Kulinowski, K. M. *Proc. Natl. Acad. Sci. U.S.A.* **2007**, *104*, 8679–8680.
- (14) Gessner, A.; Lieske, A.; Paulke, B. R.; Muller, R. H. *Eur. J. Pharm. Biopharm.* **2002**, *54*, 165–170.
- (15) Derfus, A. M.; Chan, W. C. W.; Bhatia, S. N. *Nano Lett.* **2004**, *4*, 11–18.
- (16) Cedervall, T.; Lynch, I.; Lindman, S.; Berggard, T.; Thulin, E.; Nilsson, H.; Dawson, K. A.; Linse, S. *Proc. Natl. Acad. Sci. U.S.A.* **2007**, *104*, 2050–2055.
- (17) Dobrovolskaia, M. A.; McNeil, S. E. *Nat. Nanotechnol.* **2007**, *2*, 469–478.
- (18) Gupta, A. K.; Gupta, M. *Biomaterials* **2005**, *26*, 3995–4021.
- (19) Morishita, N.; Nakagami, H.; Morishita, R.; Takeda, S.; Mishima, F.; Terazono, B.; Nishijima, S.; Kaneda, Y.; Tanaka, N. *Biochem. Biophys. Res. Commun.* **2005**, *334*, 1121–1126.
- (20) Sestier, C.; Da Silva, M. F.; Sabolovic, D.; Roger, J.; Pons, J. N. *Electrophoresis* **1998**, *19*, 1220–1226.
- (21) Vertegel, A. A.; Siegel, R. W.; Dordick, J. S. *Langmuir* **2004**, *20*, 6800–6807.
- (22) Chung, T. H.; Wu, S. H.; Yao, M.; Lu, C. W.; Lin, Y. S.; Hung, Y.; Mou, C. Y.; Chen, Y. C.; Huang, D. M. *Biomaterials* **2007**, *28*, 2959–2966.
- (23) Gan, Q.; Wang, T.; Cochrane, C.; McCarron, P. *Colloids Surf., B* **2005**, *44*, 65–73.
- (24) Lockman, P. R.; Koziara, J. M.; Mumper, R. J.; Allen, D. D. *J. Drug Targeting* **2004**, *12*, 635–641.
- (25) Pang, S. W.; Park, H. Y.; Jang, Y. S.; Kim, W. S.; Kim, J. H. *Colloids Surf., B* **2002**, *26*, 213–222.
- (26) Patil, S.; Sandberg, A.; Heckert, E.; Self, W.; Seal, S. *Biomaterials* **2007**, *28*, 4600–4607.
- (27) Bertholon, I.; Vauthier, C.; Labarre, D. *Pharm. Res.* **2006**, *23*, 1313–1323.
- (28) Hu, Y.; Xie, J. W.; Tong, Y. W.; Wang, C. H. *J. Controlled Release* **2007**, *118*, 7–17.
- (29) Prabha, S.; Zhou, W. Z.; Panyam, J.; Labhasetwar, V. *Int. J. Pharm.* **2002**, *244*, 105–115.
- (30) Win, K. Y.; Feng, S. S. *Biomaterials* **2005**, *26*, 2713–2722.
- (31) Dumortier, H.; Lacotte, S.; Pastorin, G.; Marega, R.; Wu, W.; Bonifazi, D.; Briand, J. P.; Prato, M.; Muller, S.; Bianco, A. *Nano Lett.* **2006**, *6*, 1522–1528.
- (32) Kostarelos, K.; Lacerda, L.; Pastorin, G.; Wu, W.; Wieckowski, S.; Luangsivilay, J.; Godefroy, S.; Pantarotto, D.; Briand, J. P.; Muller, S.; Prato, M.; Bianco, A. *Nat. Nanotechnol.* **2007**, *2*, 108–113.
- (33) Nakayama-Ratchford, N.; Bangsaruntip, S.; Sun, X. M.; Welsch, K.; Dai, H. J. *J. Am. Chem. Soc.* **2007**, *129*, 2448–2449.
- (34) Isobe, H.; Tanaka, T.; Maeda, R.; Noiri, E.; Solin, N.; Yudasaka, M.; Iijima, S.; Nakamura, E. *Angew. Chem., Int. Ed.* **2006**, *45*, 6676–6680.
- (35) Schellenberger, E. A.; Reynolds, F.; Weissleder, R.; Josephson, L. *ChemBioChem* **2004**, *5*, 275–279.
- (36) Weissleder, R.; Kelly, K.; Sun, E. Y.; Shtatland, T.; Josephson, L. *Nat. Biotechnol.* **2005**, *23*, 1418–1423.
- (37) Sun, E. Y.; Josephson, L.; Kelly, K. A.; Weissleder, R. *Bioconjugate Chem.* **2006**, *17*, 109–13.
- (38) Akinc, A.; Lynn, D. M.; Anderson, D. G.; Langer, R. *J. Am. Chem. Soc.* **2003**, *125*, 5316–5323.
- (39) Levy, R.; Thanh, N. T. K.; Doty, R. C.; Hussain, I.; Nichols, R. J.; Schiffrin, D. J.; Brust, M.; Fernig, D. G. *J. Am. Chem. Soc.* **2004**, *126*, 10076–10084.
- (40) Azamian, B. R.; Coleman, K. S.; Davis, J. J.; Hanson, N.; Green, M. L. H. *Chem. Commun.* **2002**, 366–367.
- (41) Drain, L. E. *Proc. Phys. Soc.* **1962**, *80*, 1380–1382.
- (42) Doskočilová, B.; Schneider, B. *Chem. Phys. Lett.* **1970**, *6*, 381–384.
- (43) Karajanagi, S. S.; Vertegel, A. A.; Kane, R. S.; Dordick, J. S. *Langmuir* **2004**, *20*, 11594–11599.
- (44) Lynch, I.; Dawson, K. A.; Linse, S. *Sci. STKE* **2006**, pe14.
- (45) Ameller, T.; Marsaud, R.; Legrand, P.; Gref, R.; Barratt, G.; Renoir, J. M. *Pharm. Res.* **2003**, *20*, 1063–1070.
- (46) Owens, D. E.; Peppas, N. A. *Int. J. Pharm.* **2006**, *307*, 93–102.
- (47) Mu, Q.; Liu, W.; Xing, Y.; Zhou, H.; Li, Z.; Zhang, Y.; Ji, L.; Wang, F.; Si, Z.; Zhang, B.; Yan, B. *J. Phys. Chem. C* **2008**, in press.
- (48) Matsuura, K.; Saito, T.; Okazaki, T.; Ohshima, S.; Yumura, M.; Iijima, S. *Chem. Phys. Lett.* **2006**, *429*, 497–502.
- (49) Adkins, J. N.; Varnum, S. M.; Auberry, K. J.; Moore, R. J.; Angell, N. H.; Smith, R. D.; Springer, D. L.; Pounds, J. G. *Mol. Cell Proteomics* **2002**, *1*, 947–955.
- (50) Worle-Knirsch, J. M.; Pulskamp, K.; Krug, H. F. *Nano Lett.* **2006**, *6*, 1261–1268.
- (51) Pulskamp, K.; Diabate, S.; Krug, H. F. *Toxicol. Lett.* **2007**, *168*, 58–74.
- (52) Green, L. C.; Wagner, D. A.; Glogowski, J.; Skipper, P. L.; Wishnok, J. S.; Tannenbaum, S. R. *Anal. Biochem.* **1982**, *126*, 131–138.

NL0730155